

Parallel In-Memory Evaluation of Spatial Joins*

Dimitrios Tsitsigkos

Information Management Systems Institute
Athena RC, Athens, Greece
dtsitsigkos@imis.athena-innovation.gr

Nikos Mamoulis

Department of Computer Science and Engineering
University of Ioannina, Greece
nikos@cs.uoi.gr

Panagiotis Bouros

Institute of Computer Science
Johannes Gutenberg University Mainz, Germany
bouros@uni-mainz.de

Manolis Terrovitis

Information Management Systems Institute
Athena RC, Athens, Greece
mter@imis.athena-innovation.gr

ABSTRACT

The spatial join is a popular operation in spatial database systems and its evaluation is a well-studied problem. As main memories become bigger and faster and commodity hardware supports parallel processing, there is a need to revamp classic join algorithms which have been designed for I/O-bound processing. In view of this, we study the in-memory and parallel evaluation of spatial joins, by re-designing a classic partitioning-based algorithm to consider alternative approaches for space partitioning. Our study shows that, compared to a straightforward implementation of the algorithm, our tuning can improve performance significantly. We also show how to select appropriate partitioning parameters based on data statistics, in order to tune the algorithm for the given join inputs. Our parallel implementation scales gracefully with the number of threads reducing the cost of the join to at most one second even for join inputs with tens of millions of rectangles.

KEYWORDS

Spatial join, in-memory data management, parallel processing, multi-core

1 INTRODUCTION

The spatial join is a well-studied fundamental operation that finds application in spatial database systems [10] and Geographic Information Systems (GIS) [17]. GIS, for example, typically store multiple thematic layers (e.g., road network, hydrography), which are spatially joined in order to find object pairs (e.g., roads and rivers) that intersect. Spatial joins are also used to support data mining operations such as clustering [9] and pattern detection [6].

Given two collections R and S of spatial objects, the objective of the *spatial intersection join* is to find pairs (r, s) , such that $r \in R$, $s \in S$ and r and s have at least one common point. Given the potentially complex geometry of the objects, intersection joins are typically processed in two steps. The *filter* step applies on spatial approximations of the objects, typically *minimum bounding rectangles* (MBRs). For each pair of object MBRs that intersect, the object geometries are fetched and compared in a *refinement step*. Similar to the vast majority of previous work [12], in this paper, we focus on the filter step. Spatial intersection join algorithms can also be used for spatial distance joins between pointsets, where the refinement step is trivial. In particular, for an ϵ -distance join, each point p is replaced (on-the-fly) by a square of side ϵ centered at p ; for each

pair of intersecting squares, we can easily verify if their distance is at most ϵ .

A wide range of spatial join algorithms have been proposed in the literature [3, 12]. Most of them assume that the input data are disk-based and their objective is to minimize I/O accesses during the join. Given the fact that main memories become bigger and faster, main-memory join processing has recently received a lot of attention [18]. In addition, given that commodity hardware supports parallel processing, multi-core join evaluation has also been the focus of recent research. Hence, in this paper, we focus on parallel in-memory evaluation of spatial joins on modern hardware.

Our focus is the optimization of the simple, but powerful partitioning-based spatial join (PBSM) algorithm [21]. PBSM is shown to perform well in previous studies [18] and used by most distributed spatial data management systems [1, 8, 31]. In a nutshell, both datasets are first partitioned using a regular grid; each tile (cell) of the grid gets all rectangles that intersect it. Each tile defines a smaller spatial join task. These tasks are independent and can be executed sequentially, assigned to different threads or even to different machines in distributed evaluation. The typical algorithm for processing each task is a plane sweep algorithm based on forward scans [5].

As an example, consider the two sets of object MBRs shown in Figure 1: $R = \{r_1, r_2, \dots, r_7\}$ and $S = \{s_1, s_2, \dots, s_6\}$. By partitioning the rectangles using a 3×3 grid, we create 9 independent spatial join tasks, one for each tile. Note that some rectangles may be replicated to multiple tiles, e.g., s_1 to tile (0,0) and (0,1). Because of this, some pairs of rectangles may be found to intersect each other in multiple tiles; e.g., pair (r_1, s_1) intersect in tiles (0,0) and (0,1). Outputting duplicate join pairs can be avoided by reporting a pair of rectangles only if a pre-determined reference point (typically, the top-left corner) of the intersection region is in the tile [7]. For example, (r_1, s_1) is only reported by tile (0,0).

Most previous works do not focus on optimizing the performance of PBSM. In particular, there is no comprehensive study so far on how the number and type of partitions should be defined. In this paper, we evaluate a 1D partitioning that divides the space into stripes, as opposed to the classic 2D partitioning, which uses a grid. Further, we investigate, for each partition, the identification of best direction of the sweep line. Finally, we show how both the partitioning and the joining phases of the algorithm can be parallelized.

*Extended version of the ACM SIGSPATIAL'19 paper under the same title.

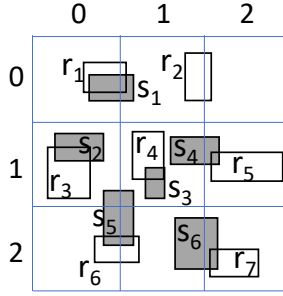


Figure 1: Example of PBSM

Based on our experimental findings, the 1D partitioning results in a more efficient algorithm. In addition, increasing the number of partitions improves the performance of the algorithm, up to a point where adding more partitions starts having a negative effect. We present a number of empirical rules driven from data statistics (globally and locally for each partition) that can guide the selection of the algorithm’s parameters. Finally, we evaluate the performance of the parallel version of the algorithm and show that it scales gracefully with the number of cores. Overall, our optimized and scalable implementation is orders of magnitude faster compared to a straightforward implementation. For example, we can perform a $8.4M \times 10M$ join in less than a second with 5 threads, which is 1-2 orders of magnitude improvement compared to the times for joining data of similar scale reported in recent work [20, 22, 26, 28–30].

The rest of the paper is organized as follows. Section 2 introduces the building blocks of PBSM and presents related work. Section 3 presents the directions along which we tune the performance of the algorithm. In Section 4, we present our evaluation on big real-world datasets. Finally, Section 5 concludes the paper and gives directions for future research.

2 BACKGROUND AND RELATED WORK

In this section, we review classic spatial join evaluation approaches and more recent work for in-memory and distributed evaluation of spatial joins. In general, in order to join spatially two large object collections R and S , we first divide them into partitions which are small enough and then join the partitions. We may also exploit an existing partitioning or index. In either case, the join is broken down into numerous small problems that can be solved fast in memory. We first discuss how a (small) join problem can be processed in memory, using a plane sweep algorithm. Then, we review how data partitioning and indexing approaches can be used to process bigger spatial join problems. Finally, we review existing work in parallel and distributed spatial join evaluation.

2.1 Evaluating Small Joins

For in-memory processing of small spatial joins, a typical approach is to use adaptations of a plane sweep algorithm that compute rectangle intersections [24]. The most commonly used adaptation was suggested by Brinkhoff et al. [5]. Algorithm 1 describes this method. The join inputs R and S are first sorted based on their lowest value in one dimension (e.g., x_l of the x -dimension). Then, the sorted inputs are scanned concurrently and merged as in a

ALGORITHM 1: Forward Scan based Plane Sweep

Input : collections of rectangles R and S
Output : set J of all intersecting rectangles $(r, s) \in R \times S$

- 1 **sort** R and S by lower x -endpoint x_l ;
- 2 $r \leftarrow$ first rectangle in R ;
- 3 $s \leftarrow$ first rectangle in S ;
- 4 **while** R and S not depleted **do**
- 5 **if** $r.x_l < s.x_l$ **then**
- 6 $s' \leftarrow s$;
- 7 **while** $s' \neq \text{null}$ and $r.x_u \geq s'.x_l$ **do**
- 8 **if** $r.y$ intersects $s'.y$ **then**
- 9 **output** (r, s') ; \triangleright update result
- 10 $s' \leftarrow$ next rectangle in S ; \triangleright scan forward
- 11 $r \leftarrow$ next rectangle in R ;
- 12 **else**
- 13 $r' \leftarrow r$;
- 14 **while** $r' \neq \text{null}$ and $s.x_u \geq r'.x_l$ **do**
- 15 **if** $r'.y$ intersects $s.y$ **then**
- 16 **output** (r', s) ; \triangleright update result
- 17 $r' \leftarrow$ next rectangle in R ; \triangleright scan forward
- 18 $s \leftarrow$ next rectangle in S ;

merge-join. This resembles a line that (is perpendicular to and) sweeps along the sorting dimension. For every value that the line encounters, say the lower x -endpoint $r.x_l$ of a rectangle $r \in R$, the other input, i.e., S , is *forwardly scanned* from the current rectangle $s' = s$, while $s'.x_l$ is *not greater than* the upper x -endpoint $r.x_u$ of r . All $s' \in S$ found in this scan are guaranteed to x -intersect r , so for each of them a y -intersection test is applied (Line 8) to confirm whether r and s' intersect. Arge et al. [2] studied more classic (but less simple to implement) versions of plane sweep based on maintenance of *active lists* at every position of the sweep line, which have insignificant performance differences to Algorithm 1.

2.2 Data Partitioning

Spatially joining large inputs directly using Algorithm 1, without any preprocessing can be quite expensive. Some 20 years ago, the memories were too small to entirely fit the input data; hence, expensive sorting and sweeping would have to be performed in external memory. Given this, *data partitioning* has been considered as a divide-and-conquer approach which splits the two inputs into smaller subsets that can then be spatially joined fast in memory. In a nutshell, each object collection is divided into a number of partitions, such that objects that are spatially close to each other fall in the same partition. A partition from R is then joined with a partition from S if their MBRs intersect.

A large number of spatial join algorithms that follow this paradigm have been proposed. They can be classified into *single-assignment*, *multi-join* (SAMJ) methods and *multi-assignment*, *single-join* (MASJ) approaches [16]. SAMJ methods assign each object to exactly one partition; the partitions are determined by spatial clustering heuristics. A partition from one dataset (e.g., R) may have

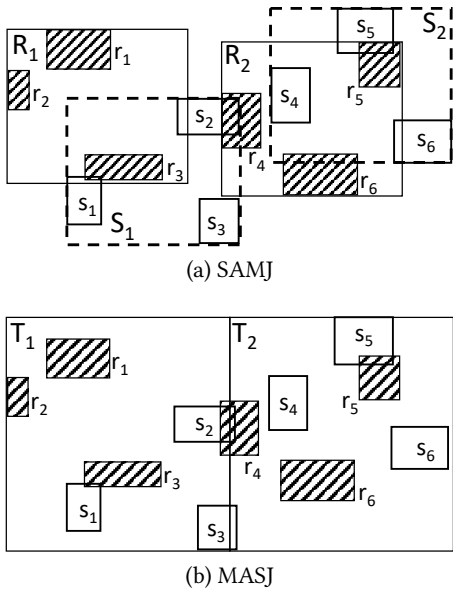


Figure 2: Two classes of partitioning techniques

to be joined with multiple partitions of the other dataset (e.g., S). In MASJ, the borders of the partitions are pre-determined, and an object is assigned to every partition it spatially intersects. Each partition from R is then joined with exactly one partition from S (which has exactly the same MBR). Figure 2 shows the differences between these two partitioning schemes. In SAMJ, illustrated in Figure 2(a), the (dark grey) rectangles of dataset R are divided to partitions R_1 and R_2 , while the (hollow) rectangles of S are divided into groups S_1 and S_2 . Partition R_1 only needs to be joined with S_1 because the MBR of R_1 does not intersect the MBR of S_2 . However, R_2 should be joined with both S_1 and S_2 . In MASJ, illustrated in Figure 2(b), the datasets are partitioned based on the space division defined by tiles T_1 and T_2 . The rectangles from R that intersect a tile (e.g., T_1) only have to be joined with the rectangles from S that are assigned to the same tile. Note that objects $\{r_4, s_2, s_3\}$, which intersect both tiles, are replicated.

A classic SAMJ approach, used when the two inputs are indexed by R-trees [11], is the *R-tree join* (RJ) algorithm of [5]. RJ finds all pairs of entries (e_R, e_S) one from each root node of the trees that intersect. For each such pair, it recursively applies the same procedure for the nodes pointed by e_R and e_S , until pairs of leaf node entries (which correspond to intersecting object MBRs) are found. For example, if R_1 and R_2 (S_1 and S_2 , respectively) in Figure 2(a) are the two children of an R-tree root that indexes R (S , respectively), then RJ would use their MBRs to determine that R_1 only needs to be joined with S_1 . Another SAMJ approach that does not rely on pre-defined indexes is *Size Separation Spatial Join* [14].

The most popular MASJ approach is *Partition-based Spatial Merge Join* (PBSM) [21]. PBSM divides the space by a regular grid and objects from both join inputs are assigned to all tiles which spatially overlap them. For example, in Figure 2(b), T_1 and T_2 could be tiles in a large rectangular grid that can be used to partition both R and S . For each partition, PBSM accesses the objects from R , the objects

from S and performs their join in memory (e.g., using plane-sweep). Since two replicated objects may intersect in multiple tiles (e.g., see r_4 and s_2 in Figure 2(b)), duplicate results may be produced. In order to avoid duplicates, a join result is reported by a tile only a pre-specified reference point (e.g., the top-left corner) of the intersection region is in the tile [7]. Other MASJ approaches include *Spatial Hash Join* [16] and *Scalable Sweeping-Based Spatial Join* [2].

More recent spatial join algorithms consider the potential differences between the joined datasets in the distribution and density. Motivated by a neuroscience application, which requires joining datasets of contrasting density, Pavlovic et al. [23] design a spatial join algorithm that partitions the dense dataset and ‘crawls’ through the partitions guided by the object locations in the sparse dataset, skipping partitions that do produce any results. Based on the same motivation, a more sophisticated approach was proposed in [22], which adapts the type of partitioning (MASJ or SAMJ) and the join technique used locally, depending on differences in the densities of the two inputs.

2.3 In-Memory Evaluation

Even with a large main memory that can accommodate the data, plane sweep can be too expensive if directly applied. The main reason behind this is that on a large map containing relatively small rectangles, the chances that two rectangles with intersecting x -projections also intersect in the y -dimension are low. Hence, plane sweep finds too many candidate pairs that x -intersect but do not materialize to actual results.

As a result, in-memory join approaches also consider data partitioning or indexing to accelerate processing. For example, as in PBSM, a grid can be used to break the problem into numerous small instances that can be solved fast. Algorithm *TOUCH* [19] is an effort in this direction, designed for scientific applications that join huge datasets that have different density and skew. TOUCH first bulk-loads an R-tree for one of the inputs using the STR technique [15]. Then, all objects from the second input are assigned to buckets corresponding to the non-leaf nodes of the tree. Each object is hashed to the lowest tree node, whose MBR overlaps it, but no other nodes at the same tree level do. Finally, each bucket is joined with the subtree rooted at the corresponding node with the help of a dynamically created grid data structure for the subtree. A recent comparison of spatial join algorithms for in-memory data [18] shows that PBSM and TOUCH perform best and that the join cost depends on the data density and distribution. Tauheed et al. [27] suggest an analytical model for configuring the grid of PBSM-like join processing in main memory; however, this model (i) assumes a nested loops evaluation of each partition-partition join and (ii) does not consider using the duplicate avoidance approach of [7].

2.4 Parallel and Distributed Evaluation

Early efforts on parallelizing spatial joins include extensions of the R-tree join and PBSM algorithms in a distributed environment of single-core processors with local storage. Consider the case of joining two R-trees. Since overlapping pairs of root entries define independent join processes for the corresponding sub-trees, these tasks can be assigned to different processors [4]. Two tasks may access a common sub-tree, therefore a virtual global buffer is shared

among processors to avoid accessing the same data twice from the disk. An early approach in parallelizing PBSM [32] asks processors to perform the partitioning of data to tiles independently and in parallel. Then, each processor is assigned one partition and processors exchange data, so that each one gets all objects that fall in its partition. The join phase is finally performed in parallel.

Recently, the research interest shifted to spatial join processing for distributed cloud systems and multi-core processors. The popularity and commercial success of the MapReduce framework motivated the development of spatial join processing algorithms on clusters. The *Spatial Join with MapReduce* (SJMP) algorithm [31] is an adaptation of the PBSM algorithm in this direction. Initially, the space is divided by a grid and tiles are grouped to partitions in a round-robin fashion after considering them in a space-filling curve order. During the *map* phase, each object is assigned to one or more partitions based on the tiles it overlaps. Each partitioned object also carries the set of tiles it intersects. Each partition corresponds to a *reduce* task. The reducers perform their joins by dividing the space that corresponds to them into stripes and performing plane sweep for each tile. Duplicate results are avoided by reporting a join pair only at the tile with the smallest id where the two objects commonly appear. In the *Hadoop-GIS* system [1] spatial joins are computed in a similar fashion. The space is divided by a grid to tiles and the objects in each tile are stored locally at nodes in the HDFS. A *global index* that is shared between nodes is used to find the HDFS files where the data of each tile are located. The local data at each node are also locally indexed. Local joins are performed by each node separately and the results are merged. The *Spatial-Hadoop* system [8] follows a similar approach where a global index per dataset is stored at a Master node, however, different datasets may have different partitioning that could pre-exist before queries. If the two join inputs are partitioned differently, then two options exist (1) use existing partitions and perform joins for every pair of partitions that overlap (they could be many) or (2) re-partition the smaller file using the same partition boundaries as the larger file and apply MASJ. The cost of each the two options is estimated and the cheapest one is selected accordingly. A query optimizer for MapReduce-based spatial join algorithms is presented in [26].

Implementations of spatial joins using Spark, where the data, indexes, and intermediate results are shared in the memories of all nodes in a cluster have also been proposed [28–30], with a focus on effective spatial indexing of the *resilient distributed datasets* (RDDs) that are generated during the process. Processing spatial joins in parallel with a focus on minimizing the cost of the refinement step was studied by Ray et al. [25]. During data partitioning, the exact geometries of objects are clipped and distributed to partitions (that may be handled by different nodes) in order to avoid any communication between nodes when object pairs whose MBRs intersect are refined. Pandey et al. [20] conducted an experimental evaluation between parallel and distributed spatial data management systems where, among other queries, spatial joins were tested. A recent piece of related work [13] studies the join between streaming points and static polygons focusing on accelerating the refinement step using modern hardware.

3 TUNING PBSM

As discussed in the previous section, the most popular spatial join framework follows the multi-assignment, single-join (MASJ) paradigm of PBSM. The reasons behind this can be summarized as follows:

- PBSM does not assume any preprocessing or indexing of the data before the join, hence it can be applied on dynamically generated spatial data.
- The partitions define independent join tasks that can easily be distributed and/or parallelized.
- The number of join tasks is the same as the number of partitions (as opposed to the number of join tasks of SAMJ approaches which can be much higher).
- Producing duplicate results can be easily avoided.
- Implementing this approach is fairly easy.
- Previous studies [18] have shown that the performance of PBSM can hardly be beaten by more sophisticated approaches based on indexing or adaptive partitioning.

In this section, we explore the directions along which we can tune PBSM in order to improve its performance. These include determining the number and type of partitions (tiles or stripes), considering alternative duplicate avoidance mechanisms, and choosing the axis along which we perform plane sweep in each partition. We also study the flexibility that these directions give to balancing the computation load in parallel spatial join evaluation. In Section 4, we evaluate the effect that all these parameters have in the performance of the algorithm when joining big spatial datasets.

3.1 One-dimensional Partitioning

The default partitioning approach followed by PBSM is by a 2D grid, as shown in Figure 1. Still, the same algorithm can be applied if we partition the data space in 1D *stripes*, as shown in Figure 3. The stripes can be horizontal or vertical. Such a partitioning has already been considered by an *external memory plane sweep* join algorithm [2]; however, the objective of the partitioning there was to define the stripes in a way such that the “horizon” of the sweep line (which runs along the axis of the stripes) fits in memory. That is, the goal of partitioning was that the *active* sets of rectangles during a stripe-to-stripe plane sweep join is small enough to fit in memory. Since in this paper, we deal with in-memory joins, we do not consider this factor, but we study how the number of partitions affects the computational cost of the spatial join (as we do for the 2D partitioning case).

3.2 Duplicate Elimination

Dittrich and Seeger [7] presented a simple but effective approach for eliminating duplicate results in PBSM. A rectangle pair is reported by a partition-partition join only if the top-left corner of their intersection area is inside the spatial extent of the partition. For example, consider the join of Figure 1. The pair of intersecting rectangles (r_1, s_1) can be found in both tiles $(0,0)$ and $(0,1)$. However, the result will only be reported in tile $(0,0)$, which contains the top-left corner of the intersection. In other words, the join result will be computed in tile $(0,1)$ but not reported. Hence, for each rectangle pair found to intersect, a *duplicate* test is performed. Let $[r.x_l, r.x_u]$ and $[r.y_l, r.y_u]$ be the projections of rectangle r on the

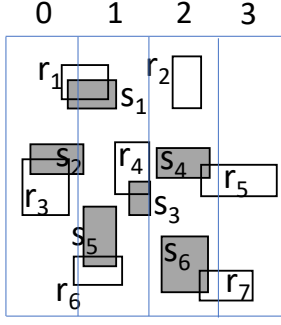


Figure 3: Example of 1D partitioning

x and y axis, respectively. Let $[T.x_l, T.x_u]$ and $[T.y_l, T.y_u]$ be the corresponding projections of a tile. The duplicate test for pair (r, s) , found to intersect in tile T , is the condition:

$$\max\{r.x_l, s.x_l\} \geq T.x_l \wedge \max\{r.y_l, s.y_l\} \geq T.y_l \quad (1)$$

Application to 1D partitioning. For the case of 1D partitioning, the duplicate test needs to apply a single comparison (as opposed to the two comparisons of Eq. 1). For example, if the stripes are vertical (as in Figure 3), a join result is reported only if $\max\{r.x_l, s.x_l\} \geq T.x_l$.

3.3 Choosing the Sweeping Axis

When applying plane sweep for a tile (or stripe) T , we have to decide along which axis we will sort the rectangles and then sweep them. As we will show in Section 4 choosing the proper axis can make a difference. For this purpose, we devise a model which, given the sets of rectangles R_T, S_T that are assigned to tile T , determines the sweeping axis to be used. The key idea is to estimate, for each axis, how many pairs of rectangles from $R_T \times S_T$ intersect along this axis. For example, if the sweeping axis is x , according to Algorithm 1, rectangle pairs that x -intersect, are essentially *candidate* or *intermediate* results; the algorithm must then verify in Line 8 or 15 if their y -projections also intersect. Hence, choosing as sweeping axis the one which produces the smallest number of candidates pairs, can reduce the cost of plane sweep.

To estimate the number of intersecting projections per axis, we compute histogram statistics. In specific, we sub-divide the x and y projections of the tile T into a predefined number of partitions k . Then, we count how many rectangles from R and how many from S , x -intersect each x -division of the tile; the procedure for y partitions is symmetric. In this manner, we construct four histograms $H_R^x, H_R^y, H_S^x, H_S^y$ of k buckets each. The number I_T^x of rectangles in $R_T \times S_T$ that x -intersect can then be approximated by accumulating the product of the corresponding histogram buckets, i.e.,

$$I_T^x = \sum_{i=0}^k \{H_R^x[i] \cdot H_S^x[i]\} \quad (2)$$

The smallest of I_T^x and I_T^y determine the chosen sweeping axis (i.e., x or y). For large tiles (compared to the size of the rectangles), we set $k = 1000$, while for small tiles k is the number of times the tile's extent is larger than the average extent of the rectangles. In practice,

it would be expensive to use all rectangles in T in the histogram construction. So, we use a sample of rectangles from R_T and S_T for this purpose. Specifically, for every ϕ rectangles that are assigned to tile T , we use one for histogram construction. We set $\phi = 100$ by default because it can produce good enough estimates at a low overhead.

Application to 1D partitioning. Our model can be straightforwardly applied in case of a 1D dimensional partitioning; histogram statistics are now computed for the contents of the vertical or horizontal stripes and the entire domain on the other dimension. However, our tests in Section 4 showed that in practice, if the partitioning axis is x , the best sweeping axis is always y and vice versa.

3.4 Parallel Processing

We parallelize evaluation by splitting each of the partitioning and joining phases of the algorithm into parallel and independent tasks, while trying to minimize the synchronization requirements between the threads. While the parallel algorithm that we outline here is designed for a single, multi-core machine, it can also be applied (with minor changes) to a cluster of machines. The steps for parallelizing the spatial join to m threads are as follows:

Partitioning phase

- (1) Determine a division of each input R and S into m equi-sized parts arbitrarily.
- (2) Initiate m threads. Thread i reads the i -th part of input R and counts how many rectangles should be assigned to each of the space partitions (tiles or stripes). Thread i repeats the same process for the i -th part of input S . Let $|R_T^i|, |S_T^i|$ be the numbers of rectangles counted by thread i for tile T and R, S , respectively.
- (3) Compute $|R_T| = \sum_i^m |R_T^i|$ and $|S_T| = \sum_i^m |S_T^i|$ for each tile T . Allocate two memory segments for $|R_T|$ and $|S_T|$ rectangles of each partition T .
- (4) Initiate m threads. Thread i reads the i -th parts of inputs R and S and partitions them. The memory allocated for each of $|R_T|$ and $|S_T|$ is logically divided into m segments based on the $|R_T^i|$'s and $|S_T^i|$'s. Hence, thread 1 will write to the first $|R_T^1|$ positions of $|R_T|$, thread 2 to the next $|R_T^2|$ positions, etc. After all threads complete partitioning, we will have the entire set of rectangles that fall in each tile continuously in memory.

Joining phase

- (5) Construct two sorting tasks for each tile T (one for R_T and one for S_T). Assign the sorting tasks to the m threads.
- (6) Construct a join task for each tile T (one for R_T and one for S_T). Assign the join tasks to the m threads.

Step 2 is applied in order to make proper memory allocation and prevent expensive dynamic allocations. It also facilitates the output of parallel partitioning for each tile T to be continuous in memory during step 4. When the model presented in Section 3.3 is used, the histograms are computed when the input data are read (i.e., in either of steps 2 and 4).

Table 1: Real datasets used in experiments

dataset	alias	cardinality	avg. x -extent	avg. y -extent
AREAWATER	$T2$	2.3M	0.000007230	0.000022958
EDGES	$T4$	70M	0.000006103	0.00001982
LINEARWATER	$T5$	5.8M	0.000022243	0.000073195
ROADS	$T8$	20M	0.000012538	0.000040672
Buildings	$O3$	115M	0.00000056	0.000000782
Lakes	$O5$	8.4M	0.000021017	0.000028236
Parks	$O6$	10M	0.000016544	0.000022294
Roads	$O9$	72M	0.000010549	0.000016281

4 EXPERIMENTAL ANALYSIS

In this section, we test the effect of the different parameters in the design of a PBSM-like spatial join. We first describe the experimental setup and then perform experiments, which test how each factor affects the performance of the algorithm and come up with empirical rules for selecting parameter values.

4.1 Setup

We experimented with a number of publicly available datasets [8].¹ For each dataset, we computed the MBRs of the objects and came up with a corresponding collection of rectangles. The datasets are normalized so that the coordinates in each dimension take values in $[0, 1]$. Table 1 provides statistics about the datasets that we used. The first three datasets are from the collection Tiger 2015 and the last three from the collection OpenStreetMap (OSM). Next to each dataset name we put a short alias indicating its order in the Tiger or OSM collection (i.e., $O3$ means the 3rd dataset from OSM). The cardinalities of the datasets range from 2.3M to 115M objects and we tested joins having inputs from the same collection, having similar or various scales. The last two columns of the tables are the relative (over the entire space) average length of the rectangle projections at each axis.

We implemented the spatial join algorithm (all different versions) in C++ and compiled it using gcc (v4.8.5) with flags `-O3`, `-mavx` and `-march=native`. For multi-threading, we used OpenMP. All experiments were run on a machine with 384 GBs of RAM and a dual 10-core Intel(R) Xeon(R) CPU E5-2630 v4 clocked at 2.20GHz running CentOS Linux 7.3.1611; with hyper-threading, we were able to run up to 40 threads. The reported runtimes include the costs of partitioning both datasets and then joining them.

4.2 Selecting Sweeping Axis

In the first experiment, we test the effect that the selection of the axis we sweep along (either x or y) has on the performance of the algorithm. For this purpose, we chose not to partition the data, but ran a single-threaded plane-sweep join using Algorithm 1 in the entire $[0, 1] \times [0, 1]$ dataspace (i.e., modeling the case of a single tile). Table 2 reports the execution times per query. We observe that sweeping along the wrong axis may even double the cost of spatial join. The last column of the table reports the details of running our model (Eq. 2). Our model was able to accurately determine the proper sweeping axis in all cases. Note that the cost of this decision-making process is negligible compared to the partitioning

¹<http://spatialhadoop.cs.umn.edu/datasets.html>

Table 2: Sweeping axis effect; queries ordered by runtime

query	sweeping axis		adaptive model	
	x	y	I^x	I^y
$T2 \bowtie T5$	8.94s	16.96s	8,376	19,232
$T2 \bowtie T8$	24.52s	40.72s	8,895	18,660
$O5 \bowtie O6$	24.92s	66.06s	2,692	12,279
$O6 \bowtie O9$	216.88s	444.19s	3,989	11,510
$T4 \bowtie T8$	674.50s	1,360.92s	8,135	19,406
$O9 \bowtie O3$	926.14s	1,681.30s	4,535	11,529

and joining cost; even for the largest queries, our model needs less than 10 milliseconds.

4.3 Evaluation of Partitioning

In the next set of experiments, we investigate the impact of partitioning to the performance of the algorithm. We first tune 1D and 2D-based PBSM and then compare the two partitioning approaches to each other.

4.3.1 Tuning 1D Partitioning. We varied the number K of (uniform) 1D partitions and for each such number, we report the cost of the algorithm for four spatial join queries in Figure 4. We tested all combinations of partitioning and sweeping axes. For example, xy denotes partitioning along the x axis (to vertical stripes) and sweeping along the y axis. We can make the following observations from the plots. First, and foremost, if the sweeping axis is the same as the partitioning axis (i.e., cases xx and yy), the join cost does not drop when we increase the number of partitions K . This is expected because, regardless the number of partitions, case xx or yy is equivalent to having no partitions at all and sweeping along the x or y axis in the entire space. When K is too large, the costs of xx and yy increase because the partitions become very narrow and replication becomes excessive. The second observation is that the performance of cases xy and yx improves with K and, after some point, i.e., $K = 2,000$, they converge to the same (very low) cost. The costs of both xy and yx starts to increase again when $K > 10,000$, at which point we start having significant replication (observe the average x - and y -extent statistics in Table 1). Figure 5 breaks down the total cost to partitioning and joining for the xy case in the range of K values where the best performance was witnessed. The cost of sorting the partition is included in the join cost. As expected, as K increases the cost of partitioning increases and the cost of the join drops, up to a point (around $K = 10,000$) after which the cost of partitioning significantly increases without providing any improvement in the performance of the join. Overall, the xy case is marginally better than the yx case and the lowest runtime is achieved when the x -extent of the partitions (i.e., the narrow side of the stripes) is about 10 times larger than the average x -extent of the rectangles. In this case, the chances that a rectangle is replicated to neighboring stripes are small and at the same time, the stripes are narrow enough for plane sweep to be effective (i.e., the chance that a candidate pair that x -intersects also y -intersects is not low). For the rest of our analysis we use xy as the default setup for 1D partitioning.

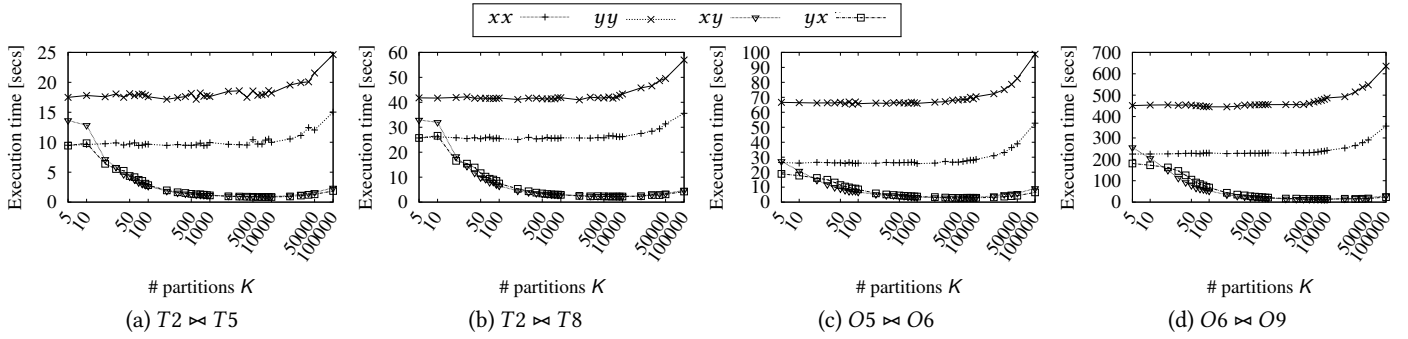


Figure 4: Tuning 1D partitioning: total execution time

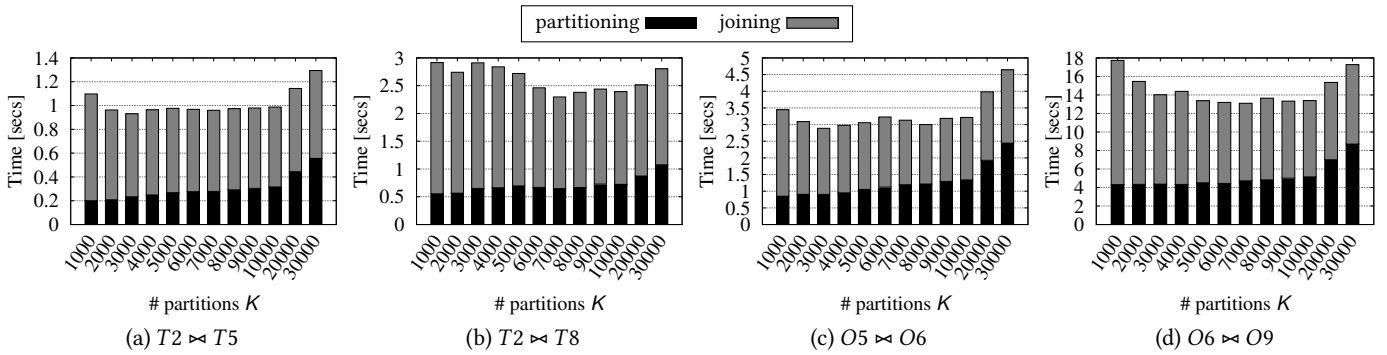


Figure 5: Tuning 1D partitioning: time breakdown

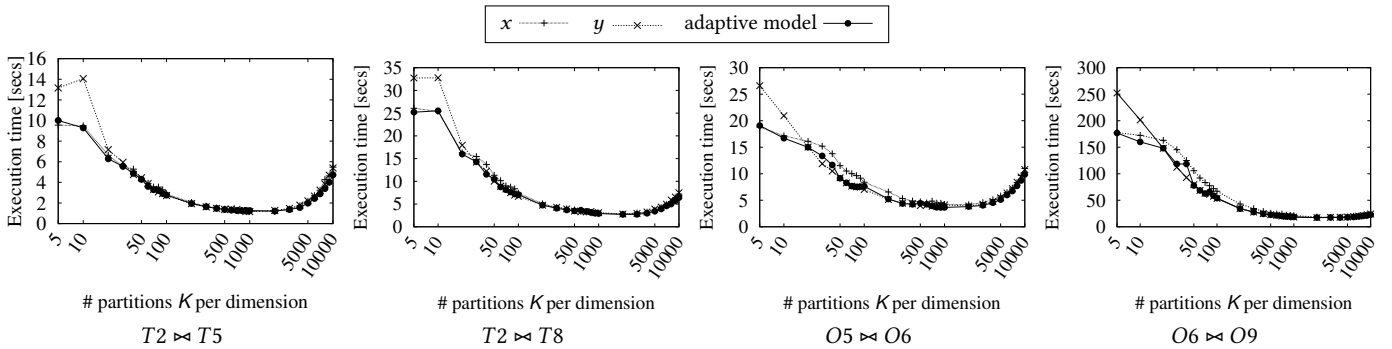


Figure 6: Tuning 2D partitioning: total execution time

4.3.2 *Tuning 2D Partitioning.* We varied the granularity $K \times K$ of the grid and measure for each value of K the runtime cost of the algorithm, when the sweeping axis is always set to x , always set to y , or when our adaptive model is used to select the sweeping axis at each tile (which could be different at different tiles). Figure 6 depicts the performance of the three join variants. The observations regarding the choice of the sweeping axis and the number of partitions are similar to the cases of 1D partitioning. Specifically, when the number of partitions is small $K \leq 20$, the choice of the sweeping axis makes a difference and choosing x is better. In these configurations, our model can be even better than always choosing

x . The three options converge at about $K = 500$ and there are no significant differences between them after this point.

Figure 7 shows the cost breakdown for the partitioning and joining phases of the 2D spatial join, when our model is used for picking the sweeping axis x . As in the case of 1D joins, we observe that the cost of partitioning increases with K and becomes too high when the tiles become too many and very small (i.e., when $K > 2,000$). On the other hand, the join cost drops, but stabilizes after $K > 2,000$. After this point, the number $K \times K$ of tiles (that have to be managed) becomes significantly high and replication becomes excessive. The joining phase does not benefit; due to replication,

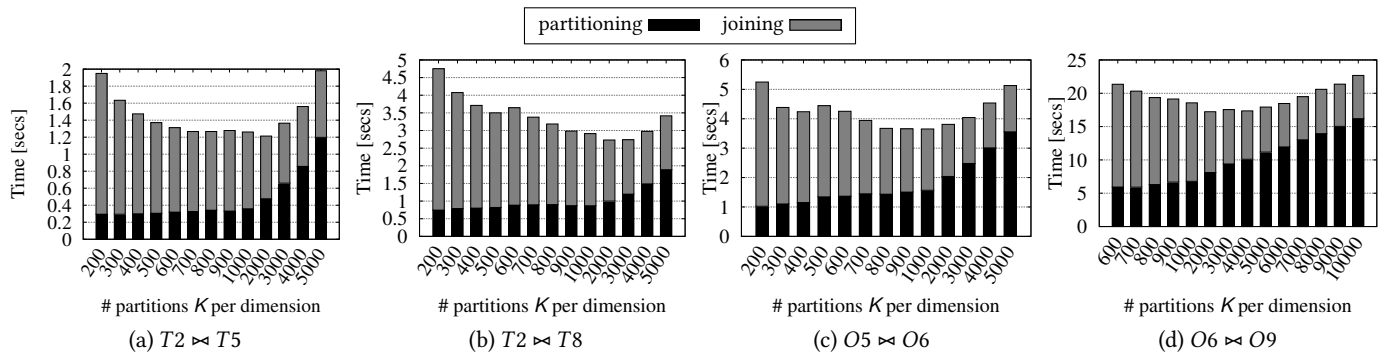


Figure 7: Tuning 2D partitioning: time breakdown

Table 3: 1D vs. 2D partitioning: speedup

query	1D		2D	
	K	speedup	$K \times K$	speedup
$T2 \leftrightarrow T5$	3000	9.6x	1000×1000	8.16x
$T2 \leftrightarrow T8$	7000	10.67x	2000×2000	8.98x
$O5 \leftrightarrow O6$	3000	8.62x	1000×1000	6.82x
$O6 \leftrightarrow O9$	7000	16.56x	2000×2000	12.58x

the join inputs at each tile do not reduce in size and the same join results are computed in neighboring tiles. To sum up, the best grid configuration is around $K = 2,000$, which is consistent with the best option in 1D partitioning. In addition, our tests show that the 2D partitioning version of the algorithm should always use our adaptive model to select the sweeping axis.

4.3.3 *1D vs. 2D Partitioning.* Our experiments in tuning PBSM draw two important observations. First, regarding the number of partitions, the rule of the thumb is to select K (in both 1D and 2D partitioning) such that the extents of the resulting partitions are about one order of magnitude larger than the extents of the rectangles (in one or both dimensions, respectively). For the rest of our analysis, we use this rule to select K as the default number of divisions in the splitting dimension(s).

Second, 1D partitioning achieves better performance compared to 2D partitioning, due to less replication and the fact that all tiles in a row or a column can be swept by a single line (along the row or column) with the same effect as processing all tiles independently with sweeping along the same direction. Table 3 summarizes, for the four join queries, the best speedups achieved by 1D and 2D partitioning, compared to the best corresponding performance of the plane sweep algorithm without partitioning. 1D partitioning is up to 32% faster compared to 2D partitioning.

4.4 Parallel Evaluation

In the last experiment, we tested the parallel version of the algorithm. We used 1D partitioning which is superior to 2D partitioning as shown in Table 3. Table 4 summarizes, for the four join queries, the runtime and the speedup achieved by our parallel evaluation of the spatial join. Note that the performance scales gracefully with the number of threads, until it stabilizes over 20 threads, which

Table 4: Parallel evaluation: runtime (1D partitioning)

# threads	queries			
	$O5 \leftrightarrow O6$	$O6 \leftrightarrow O9$	$T4 \leftrightarrow T8$	$O9 \leftrightarrow O3$
1	2.98s	14.4s	20.1s	43.0s
5	0.75s	3.32s	4.34s	10.6s
10	0.46s	1.91s	2.47s	6.11s
15	0.38s	1.45s	1.85s	4.54s
20	0.32s	1.21s	1.64s	3.54s
25	0.29s	1.07s	1.42s	3.09s
30	0.28s	0.99s	1.36s	2.89s
35	0.27s	0.96s	1.27s	2.72s
40	0.27s	0.91s	1.21s	2.72s

equals the number of physical cores in our machine. As a general conclusion our parallel design takes full advantage of the system resources to reduce the join cost in the order of a few seconds. We are not aware of any previous work that can achieve such a performance when joining datasets in the order of several millions of objects each.

5 CONCLUSIONS

In this paper, we have investigated directions towards tuning a classic and popular partitioning-based spatial join algorithm, which is typically used for in-memory and parallel/distributed join evaluation. We investigated the tuning of the algorithm by varying the number and type of partitions and the sweeping axis choice in plane sweep. We also designed an efficient parallel version of the algorithm. Our experimental findings show that 1D partitioning performs better than 2D and that the correct sweeping axis choice does matter. In addition, we showed that the parallel version of the algorithm scales well with the number of threads.

Directions for future work include consideration of the refinement step of the join, which can be significantly more expensive than the filter step. In addition, we plan to adapt our techniques and investigate their performance in a distributed environment and for the case of NUMA architectures.

REFERENCES

- [1] Abhimat Aji, Fusheng Wang, Hoang Vo, Rubao Lee, Qiaoling Liu, Xiaodong Zhang, and Joel H. Saltz. 2013. Hadoop-GIS: A High Performance Spatial Data Warehousing System over MapReduce. *PVLDB* 6, 11 (2013), 1009–1020.

- [2] Lars Arge, Octavian Procopiuc, Sridhar Ramaswamy, Torsten Suel, and Jeffrey Scott Vitter. 1998. Scalable Sweeping-Based Spatial Join. In *VLDB*. 570–581.
- [3] Panagiotis Boursos and Nikos Mamoulis. 2019. Spatial Joins: What’s next? *SIGSPATIAL Special* 11, 1 (2019), 13–21.
- [4] Thomas Brinkhoff, Hans-Peter Kriegel, and Bernhard Seeger. 1996. Parallel Processing of Spatial Joins Using R-trees. In *ICDE*. 258–265.
- [5] Thomas Brinkhoff, Hans-Peter Kriegel, and Bernhard Seeger. 1993. Efficient Processing of Spatial Joins Using R-Trees. In *SIGMOD Conference*. 237–246.
- [6] Huiping Cao, Nikos Mamoulis, and David W. Cheung. 2007. Discovery of Periodic Patterns in Spatiotemporal Sequences. *IEEE Trans. Knowl. Data Eng.* 19, 4 (2007), 453–467.
- [7] Jens-Peter Dittrich and Bernhard Seeger. 2000. Data Redundancy and Duplicate Detection in Spatial Join Processing. In *ICDE*. 535–546.
- [8] Ahmed Eldawy and Mohamed F. Mokbel. 2015. SpatialHadoop: A MapReduce framework for spatial data. In *ICDE*. 1352–1363.
- [9] Martin Ester, Hans-Peter Kriegel, Jörg Sander, and Xiaowei Xu. 1996. A Density-Based Algorithm for Discovering Clusters in Large Spatial Databases with Noise. In *Proceedings of the Second International Conference on Knowledge Discovery and Data Mining (KDD-96), Portland, Oregon, USA*. 226–231.
- [10] Ralf Hartmut Güting. 1994. An Introduction to Spatial Database Systems. *VLDB Journal* 3, 4 (1994), 357–399.
- [11] Antonin Guttman. 1984. R-Trees: A Dynamic Index Structure for Spatial Searching. In *SIGMOD Conference*. 47–57.
- [12] Edwin H. Jacox and Hanan Samet. 2007. Spatial join techniques. *ACM Transactions on Database Systems* 32, 1 (2007), 7.
- [13] Andreas Kipf, Harald Lang, Varun Pandey, Raul Alexandru Persa, Peter A. Boncz, Thomas Neumann, and Alfons Kemper. 2018. Adaptive Geospatial Joins for Modern Hardware. *CoRR* abs/1802.09488 (2018). <http://arxiv.org/abs/1802.09488>
- [14] Nick Koudas and Kenneth C. Sevcik. 1997. Size Separation Spatial Join. In *SIGMOD Conference*. 324–335.
- [15] Scott T. Leutenegger, J. M. Edgington, and Mario A. López. 1997. STR: A Simple and Efficient Algorithm for R-Tree Packing. In *ICDE*. 497–506.
- [16] Ming-Ling Lo and Chinya V. Ravishankar. 1996. Spatial Hash-Joins. In *SIGMOD Conference*. 247–258.
- [17] Paul A. Longley, Mike Goodchild, David J. Maguire, and David W. Rhind. 2010. *Geographic Information Systems and Science* (3rd ed.). Wiley Publishing.
- [18] Sadegh Nobari, Qiang Qu, and Christian S. Jensen. 2017. In-Memory Spatial Join: The Data Matters!. In *EDBT*. 462–465.
- [19] Sadegh Nobari, Farhan Tauheed, Thomas Heinis, Panagiotis Karras, Stéphane Bressan, and Anastasia Ailamaki. 2013. TOUCH: in-memory spatial join by hierarchical data-oriented partitioning. In *SIGMOD Conference*. 701–712.
- [20] Varun Pandey, Andreas Kipf, Thomas Neumann, and Alfons Kemper. 2018. How Good Are Modern Spatial Analytics Systems? *PVLDB* 11, 11 (2018), 1661–1673.
- [21] Jignesh M. Patel and David J. DeWitt. 1996. Partition Based Spatial-Merge Join. In *SIGMOD Conference*. 259–270.
- [22] Mirjana Pavlovic, Thomas Heinis, Farhan Tauheed, Panagiotis Karras, and Anastasia Ailamaki. 2016. TRANSFORMERS: Robust spatial joins on non-uniform data distributions. In *ICDE*. 673–684.
- [23] Mirjana Pavlovic, Farhan Tauheed, Thomas Heinis, and Anastasia Ailamaki. 2013. GIPSY: joining spatial datasets with contrasting density. In *SSDBM*.
- [24] Franco P. Preparata and Michael Ian Shamos. 1985. *Computational Geometry - An Introduction*. Springer.
- [25] Suprio Ray, Bogdan Simion, Angela Demke Brown, and Ryan Johnson. 2014. Skew-resistant parallel in-memory spatial join. In *SSDBM*. 6:1–6:12.
- [26] Ibrahim Sabek and Mohamed F. Mokbel. 2017. On Spatial Joins in MapReduce. In *SIGSPATIAL/GIS*.
- [27] Farhan Tauheed, Thomas Heinis, and Anastasia Ailamaki. 2015. Configuring Spatial Grids for Efficient Main Memory Joins. In *BICOD*.
- [28] Dong Xie, Feifei Li, Bin Yao, Gefei Li, Zhongpu Chen, Liang Zhou, and Minyi Guo. 2016. Simba: spatial in-memory big data analysis. In *SIGSPATIAL/GIS*. 86:1–86:4.
- [29] Simin You, Jianting Zhang, and Le Gruenwald. 2015. Large-scale spatial join query processing in Cloud. In *CloudDB, ICDE Workshops*. 34–41.
- [30] Jia Yu, Jinxuan Wu, and Mohamed Sarwat. 2015. GeoSpark: a cluster computing framework for processing large-scale spatial data. In *SIGSPATIAL/GIS*. 70:1–70:4.
- [31] Shubin Zhang, Jizhong Han, Zhiyong Liu, Kai Wang, and Zhiyong Xu. 2009. SJMR: Parallelizing spatial join with MapReduce on clusters. In *CLUSTER*. 1–8.
- [32] Xiaofang Zhou, David J. Abel, and David Truffet. 1997. Data Partitioning for Parallel Spatial Join Processing. In *SSD*. 178–196.